# Application of High Strength Woven Geotextile in Embankment Stability Control on Soft Soils

B. Wai-Choo Kok, Abigroup Pty Ltd, Australia, barry.kok@abigroup.com.au
J. Berends, Maccaferri Pty Ltd, Australia, jeroenberends@maccaferri.com.au
K. Hooi Loke, Tencate Geosynthetics Asia, Malaysia, kh.loke@tencate.com

ABSTRACT
In a fast paced construction world, the application of high strength woven geotextile as tensioned membranes to restrict the vertical displacement of ground underneath and subsequently increase the stability of road embankments is becoming more popular. Due to the relatively low permeability of soft soils, particularly clayey materials, the drainage and consolidation process is significantly slow. The road embankments need reinforcement in order to increase the soil shearing resistance before they are able to support their own weight. The main objective of this study is to quantify the effectiveness of high strength woven geotextile in stability control on soft soils in the Kedron Brook floodplain area, Brisbane. This area consists mainly of Holocene Clays up to 26m depth. More than 1,000,000m$^2$ of high strength woven geotextile has been used as reinforcement to control stability in heavily instrumented road embankments located in the Airport Interchange area of Brisbane, Australia. Lateral ground movement due to the consolidation process by fill activity were computed using 2D finite element analysis and compared to the horizontal displacement recorded by inclinometers installed along the embankments, quantified as settlement ratio. The settlement ratio ranging from 1.2 to 4.0 in reinforced embankments and 0.2 to 2.7 in unreinforced embankments. The effectiveness of high strength woven geotextile increased the settlement ratio and provided additional safety factor in stability control of road embankments on soft soil areas to improve the construction rate.

## 1. INTRODUCTION

In 1986, Queensland Motorways delivered the historic Gateway Bridge which was built at a cost of $140 million and has been heralded a great engineering triumph. The Gateway Bridge and sections of the motorway are either at, or fast approaching capacity, which necessitates a need for a new Gateway Motorway deviation and airport interchange. The $1.88 billion Gateway Upgrade Project is the largest bridge and road project in Queensland's history. It is a State Government initiative being delivered by Queensland Motorways, with design, construction and maintenance by the Leighton - Abigroup Joint Venture.

The project involves the construction of a second Gateway Bridge, the refurbishment of the existing Gateway Bridge, a 12km upgrade to the Gateway Motorway and 7km's of new motorway. Construction works commenced early 2007 with the project scheduled for completion in early 2011.

A total of sixteen bridge structures will be built for the deviation however for the purpose of this paper we will focus on the Embankments for Bridges 19B and Bridges 25A & B which incorporated the use of high strength woven geotextile.

## 2. GEOLOGICAL PROFILE DESCRIPTION

The geological sequencing of the Northern Kedron Brook and Airport Drive areas consists of the upper and lower Holocene deposits underlain by the relict Pleistocene alluvia, residual soils and rock.

The Upper Holocene alluvia were laid down during the most recent rise in sea level, in shallow fluctuating water bodies, and are comprised of interlayered clays, silts, and sands, sometimes with peaty inclusions. They are present from the ground surface (or from the base of any site fill) and are usually between 6m and 12m thick. These alluvia are highly compressible (apart from a shallow crust) but usually settle relatively rapidly.

The lower Holocene alluvia were laid down in deeper water, either off-shore or in deeper stream channels. They tend to be silty clays underlain by sandy layers and extend to significant depths; in excess of 30 m in some places. They are highly compressible, and because they lack persistent layers of sand, they consolidate relatively slowly taking years or even decades to complete primary consolidation depending on their thickness.

The underlying Pleistocene deposits generally comprise stiff to hard clayey and medium dense to very dense sandy gravely materials. Their upper profile was a former land surface, shaped by erosion and stream cutting during lower sea levels. Rock, present beneath the alluvia, consists of the Tertiary-age Petrie Formation which comprises mudstone, shale, sandstone, oil shale and pebble and cobble conglomerate.

The geological profiles of the various sections of the road embankment and the airport interchange area are shown in Figures 1 and 2. General soil properties from laboratory tests at the Airport Interchange area are provided in Figure 3.

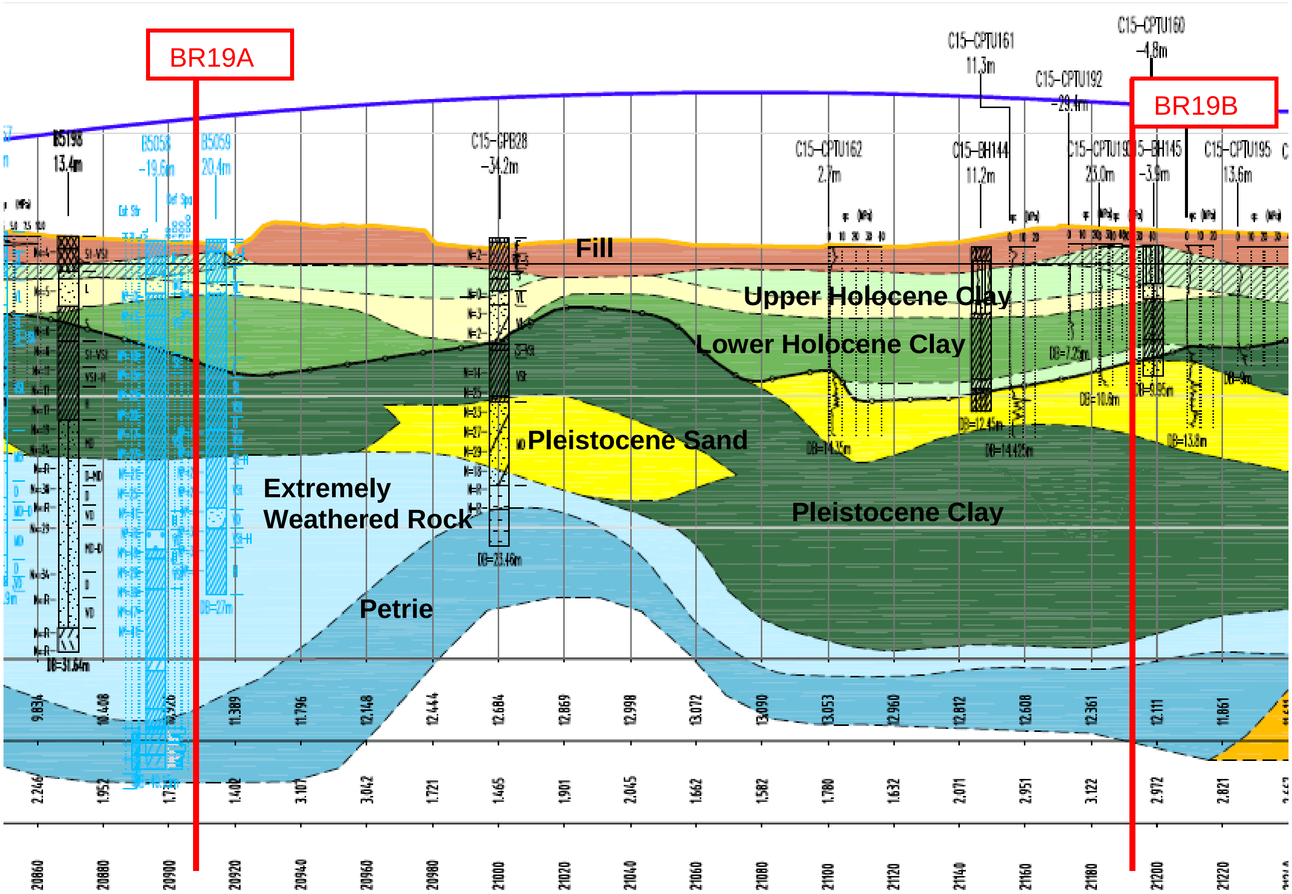


Figure 1. Geological long section profile – BR 19A & B (Coffey Report, 2007)

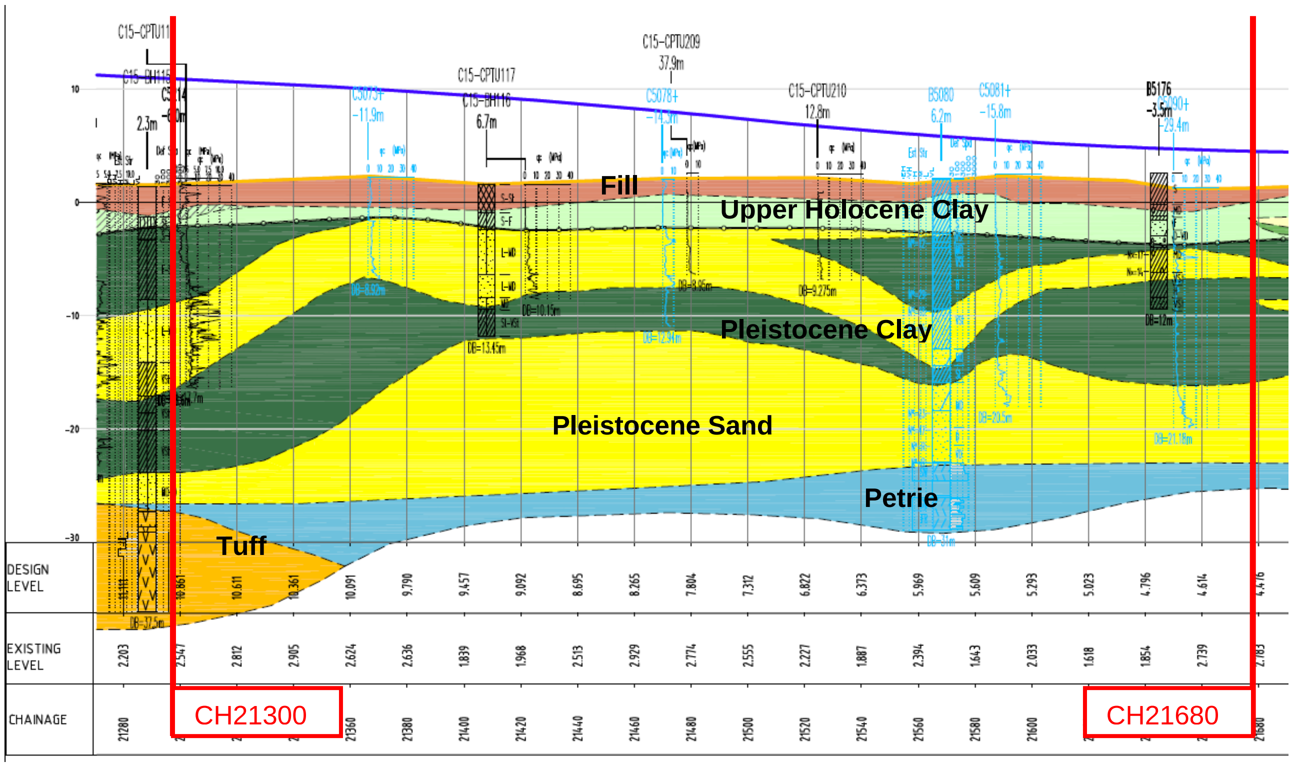


Figure 2. Geological long section profile – CH21300 & CH21680 (Coffey Report, 2007)

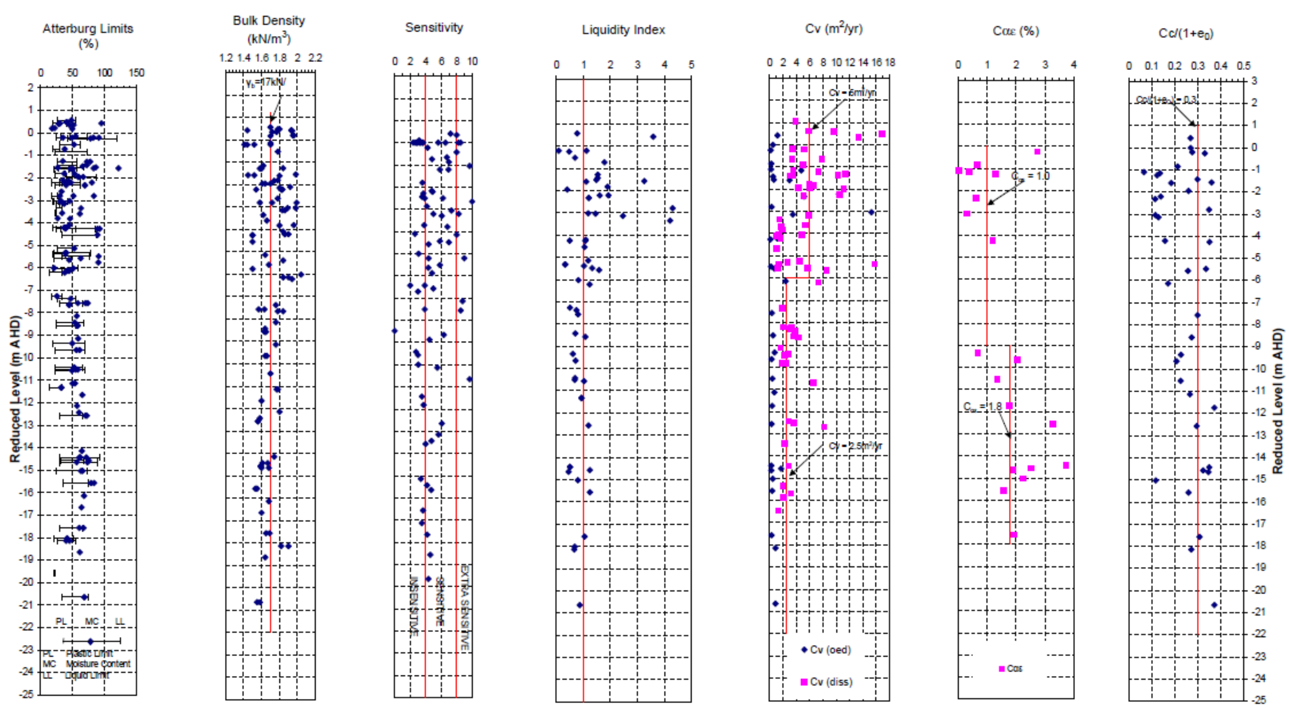


Figure 3. General soil properties from laboratory tests at Airport Interchange area (Coffey Report, 2007)

3. CONSTRUCTION METHODOLOGY

The embankments were constructed using a 300mm layer of fine silty sand placed on top of the existing alluvial crust which was then lightly compacted. Two layers of high strength woven geotextile were then placed on top of the fine silty sand layer and each layer of geotextile separated by another 300mm blanket of fine silty sand. The sand blanket maintains friction between the reinforced soil layers and minimizes construction damage. Embankment BR19B had an additional layer of high strength woven placed 6m above the toe of the embankment. To achieve the embankment design height, subsequent layers of engineered fill 1.5m deep were placed every 10 working days.

The cross sections of both geotextile reinforced and unreinforced embankments are shown in Figures 4 and 5.

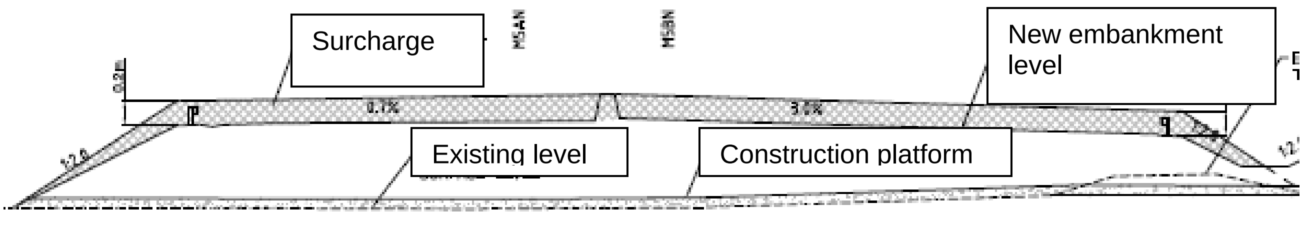


Figure 4. Typical geometry of unreinforced road embankment

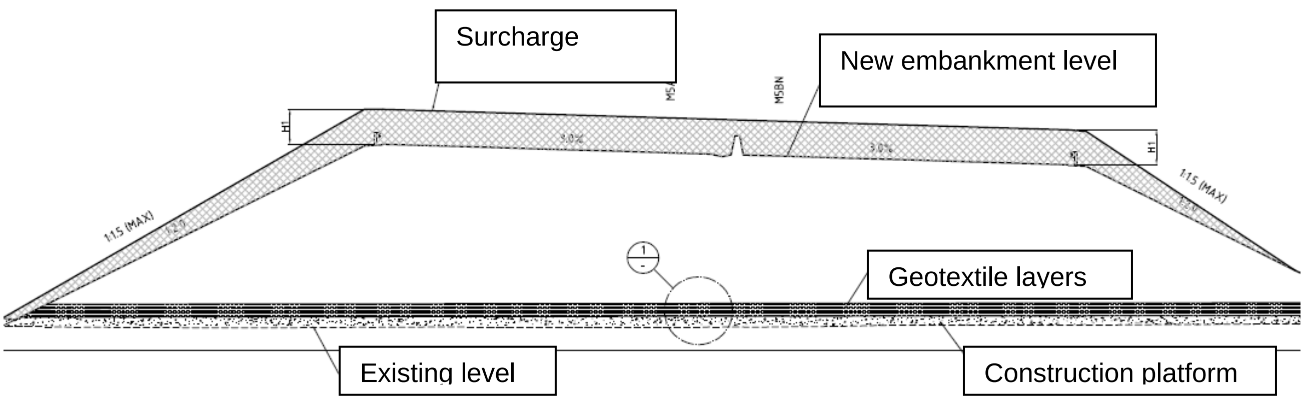


Figure 5. Typical geometry of geotextile reinforced road embankment

The table below indicates the geometry of the embankments as well as preload conditions, depths of Holocene clays and the number of high strength woven geotextile layers used at each of the embankments.

Table 1. Embankment profiles and number of high strength geotextile layers

| Area | Height of embankment (m) | Surcharge height (m) | Total height (m) | Preload period (months) | Soft clay thickness (m) | Layers of high strength woven geotextile |
|---|---|---|---|---|---|---|
| 21+300 | 9.8 | 0.5 | 10.3 | 3.0 | 1.0 | None |
| 21+680 | 2.9 | 2.1 | 5.0 | 6.0 | 6.5 | None |
| BR19B | 11.0 | 3.0 | 14.0 | 3.0 | 5.0 | 3 layers of WX 800 |
| BR25A | 4.3 | 4.3 | 8.6 | 6.0 | 20.0 | 2 layers of WX 600 |
| BR25B | 4.3 | 4.3 | 8.6 | 6.0 | 20.0 | 3 layers of WX 600 |

Inclinometers were placed at the toe of all the reinforced and unreinforced embankments in order to measure lateral movements generated by applied overburden pressure (Figure 6). Field measured values were recorded and are shown in Table 4.

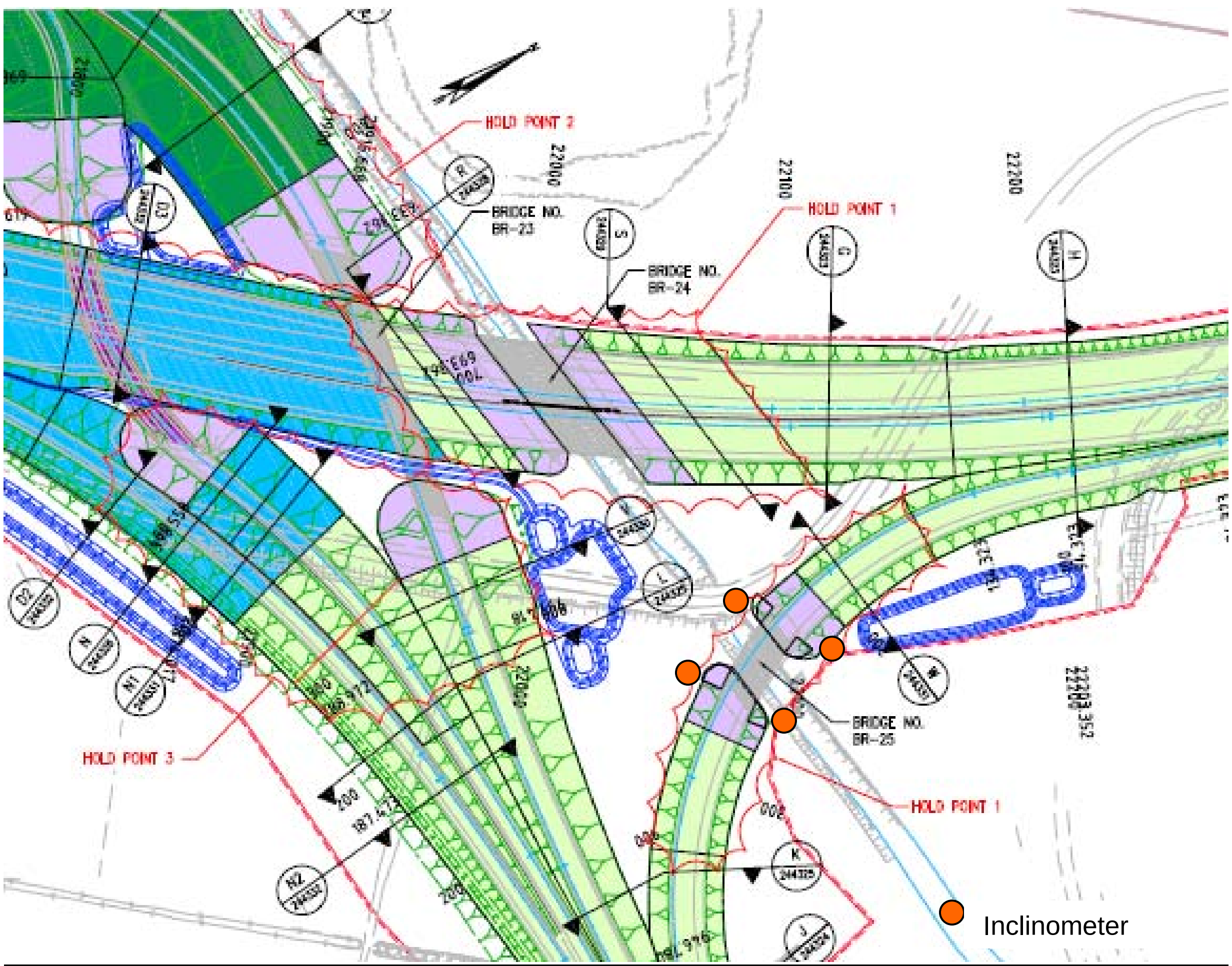


Figure 6. Plan view showing locations of inclinometers for BR25A & B

## 4. GEOSYTHETIC MATERIAL PROPERTIES

A high-strength woven geotextile (Polyfelt WX) was selected as the most appropriate geosynthetic reinforcement to ensure short and long term stability of the embankments in this project. The product is manufactured using high modulus polyester fibres which allow them to exhibit very low creep strains at high tensile load levels. The fibres are assembled to form a directionally structured and stable geotextile that enables maximum load carrying capacity and efficiency. Partial material factors were adopted to determine the long term strength characteristics under specific load and environmental regimes. These factors are shown in Table 2. Figure 7 shows the placement of the high strength geotextile at the base of the embankment.

Table 2. Mechanical properties of the high strength woven geotextiles

| Area | Product | Short term tensile strength (kN/m) | Partial factor creep ($F_c$) | Partial factor construction damage ($F_d$) | Partial factor environmental Effects ($F_e$) | Long term tensile strength (kN/m) |
|---|---|---|---|---|---|---|
| BR 19B | WX 800 | 800 | 1.55 | 1.00 | 1.1 | 469.2 |
| BR 25A | WX 600 | 600 | 1.55 | 1.00 | 1.1 | 351.9 |
| BR 25B | WX 600 | 600 | 1.55 | 1.00 | 1.1 | 351.9 |


Figure 7. The fabric installed at BR25A and BR25B

## 5. 2D FINITE ELEMENT MODELING

The 2D finite element modelling approach adopts the Mohr-Coulomb drained soil model with consolidation analysis in order to calculate the maximum horizontal displacement at the toe of the embankments. The results of the finite element analyses are shown in Figure 8 to 11.

The following parameters were adopted to model the 2D finite element analysis as shown in Table 3.

Table 3: Soil Parameters Used For 2D Finite Element Models

| Soil Type | $\gamma_{sat}$ (kN/m³) | $E_{ref}$ (kN/m²) | $C_{ref}$ (kN/m²) | $\theta$ (Degrees) | $\upsilon$ (Poisson's Ratio) |
|---|---|---|---|---|---|
| Engineered Fill | 20 | 20 000 | 5 | 30 | 0.30 |
| In Situ Fill | 16.5 | 15 000 | 1 | 30 | 0.30 |
| Alluvial Crust | 19 | 12 000 | 60 | 26 | 0.33 |
| Soft Clay | 17 | 3 750 | 20 | 20 | 0.33 |
| Stiff Clay | 17 | 25 000 | 80 | 24 | 0.33 |
| Very Stiff Clay | 18 | 30 000 | 100 | 26 | 0.33 |
| Loose Sand | 17 | 10 000 | 0 | 29 | 0.30 |
| Medium Dense Sand | 18 | 20 000 | 0 | 31 | 0.30 |
| Dense Sand | 19 | 40 000 | 1 | 33 | 0.30 |
| Gravel | 21 | 75 000 | 1 | 35 | 0.30 |

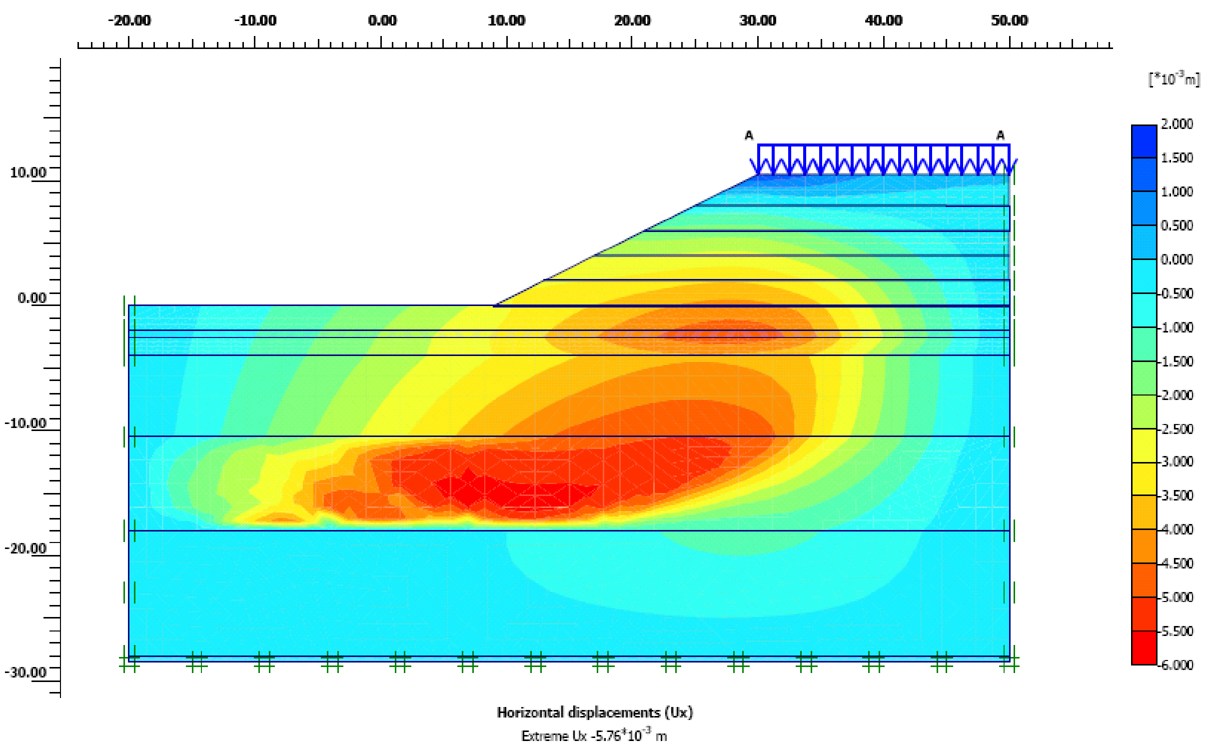


Figure 8. Results of 2D Finite Element analysis on 21+300 (unreinforced sections)

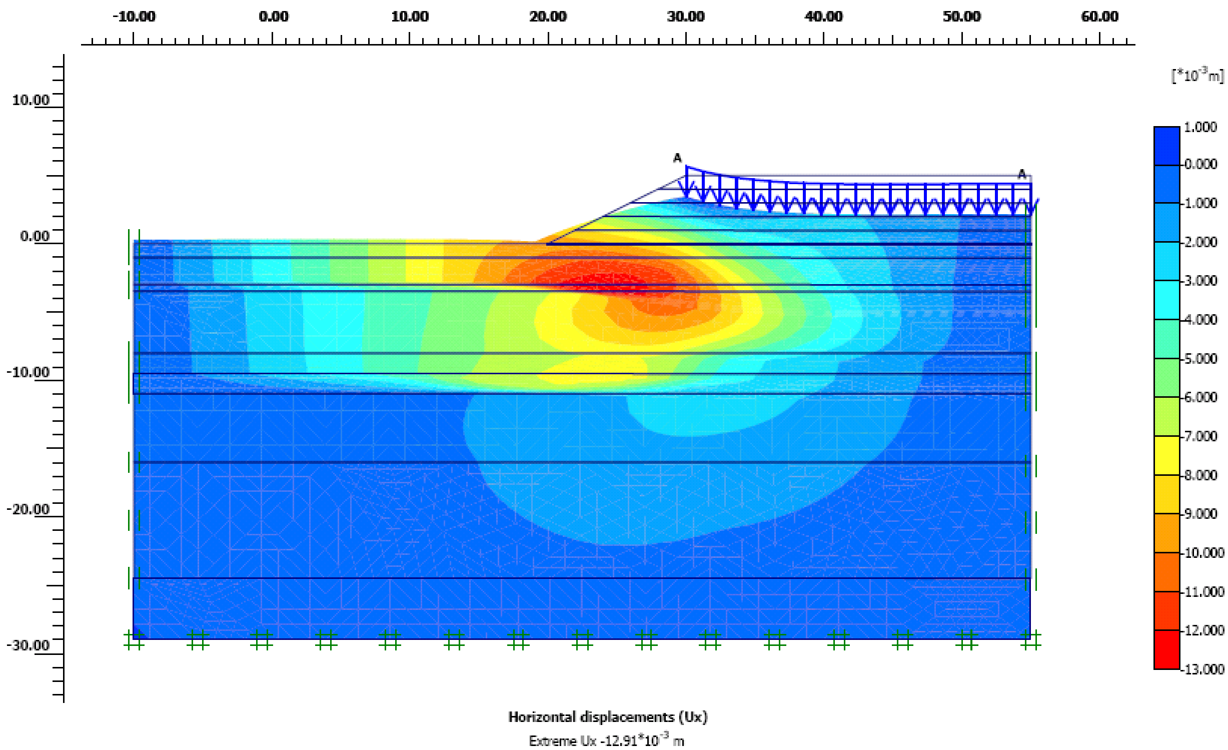


Figure 9. Results of 2D Finite Element analysis on 21+680 (unreinforced sections)

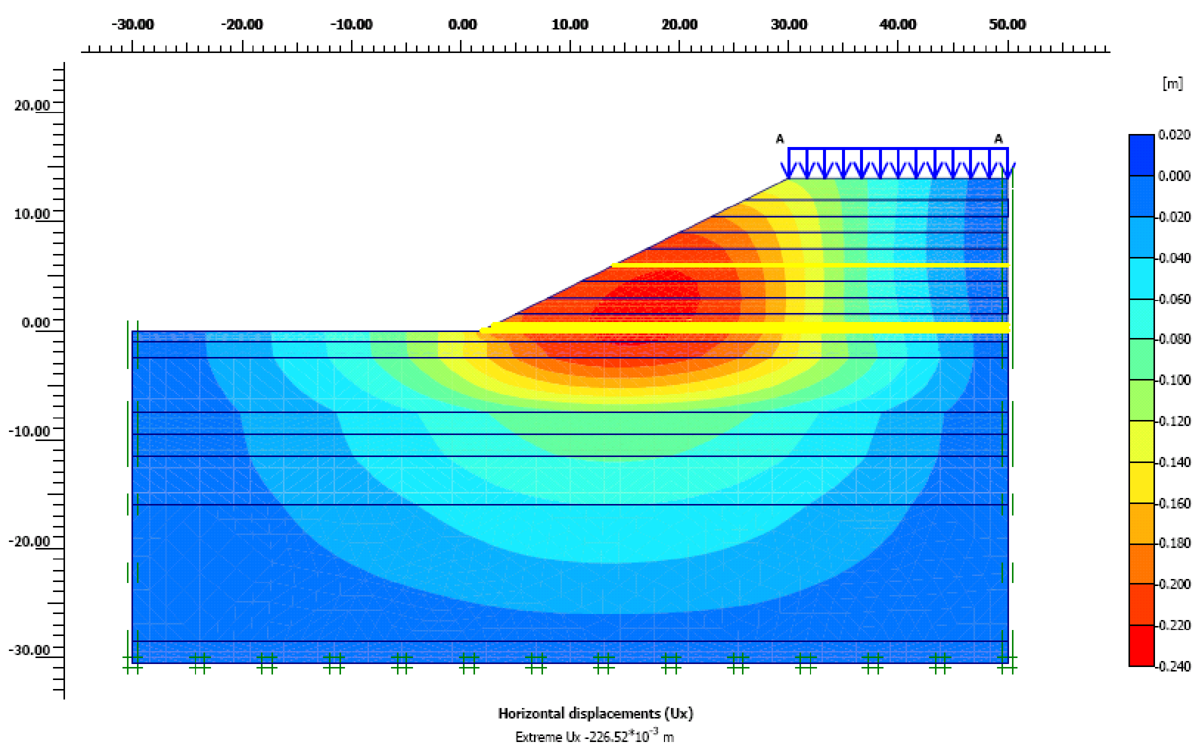

Figure 10. Results of 2D Finite Element analysis on BR19B (reinforced sections)

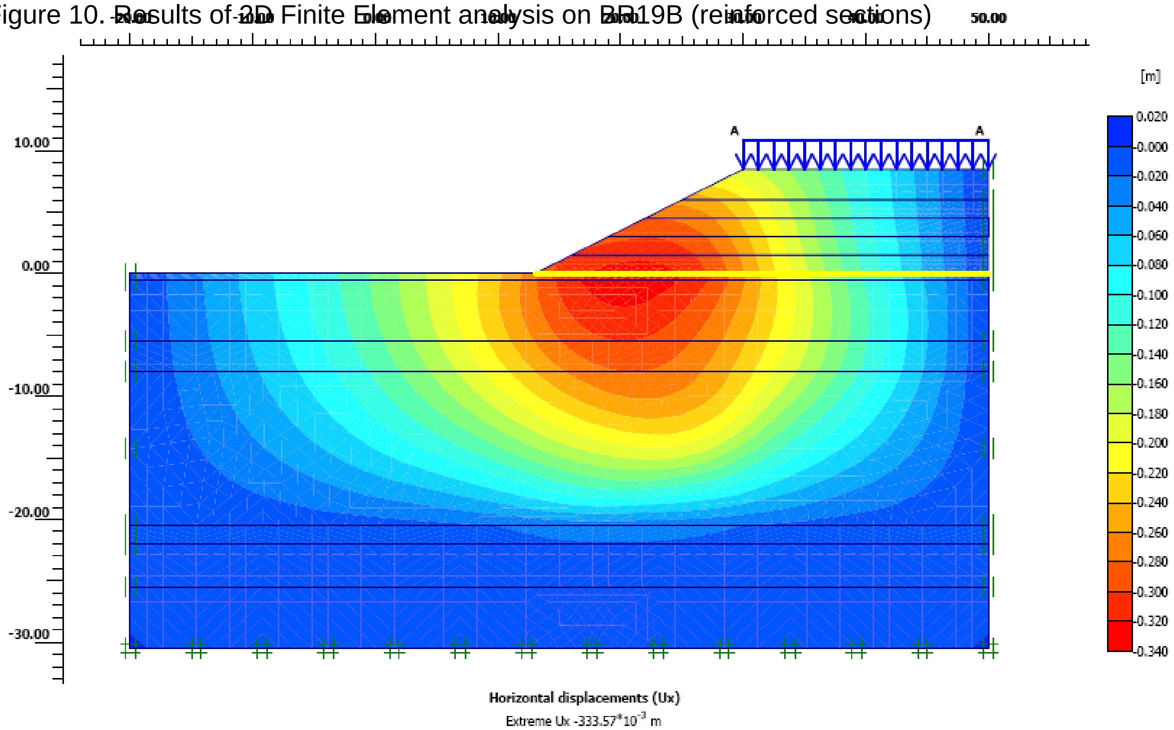


Figure 11. Results of 2D Finite Element analysis on BR25A & B (reinforced sections)

## 6. RESULTS

Table 4: 2D Finite Element Analysis Results Vs Field Measured Results

| Area | (A) 2D FEM Predicted horizontal displacement (mm) | (B) Field measured horizontal displacement (mm) | Inclinometer ID | Settlement Ratio (A / B) |
|---|---|---|---|---|
| BR19B | 178.9 | 83.6 | I44-NB | 2.1 |
| | 178.9 | 44.9 | I45-SB | 4.0 |
| BR25A | 285.3 | 113.6 | I10-NB | 2.5 |
| | 285.3 | 235.5 | I11-SB | 1.2 |
| BR25B | 285.3 | 103.6 | I12-NB | 2.8 |
| | 285.3 | 222.7 | I13-SB | 1.3 |
| 21300 | 5.7 | 26.9 | I3-NB | 0.2 |
| | 5.7 | 2.1 | I4-SB | 2.7 |
| 21680 | 11.3 | 7.0 | I13-SB | 1.6 |
| | 11.3 | 13.7 | I14-NB | 0.3 |

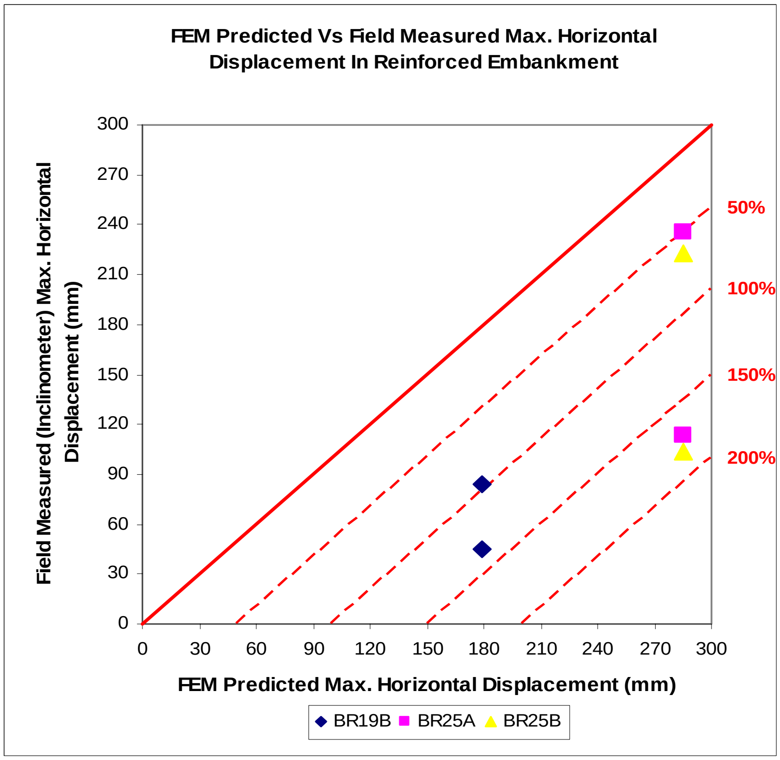


Figures 12: FEM vs Field measured horizontal displacements for reinforced embankments

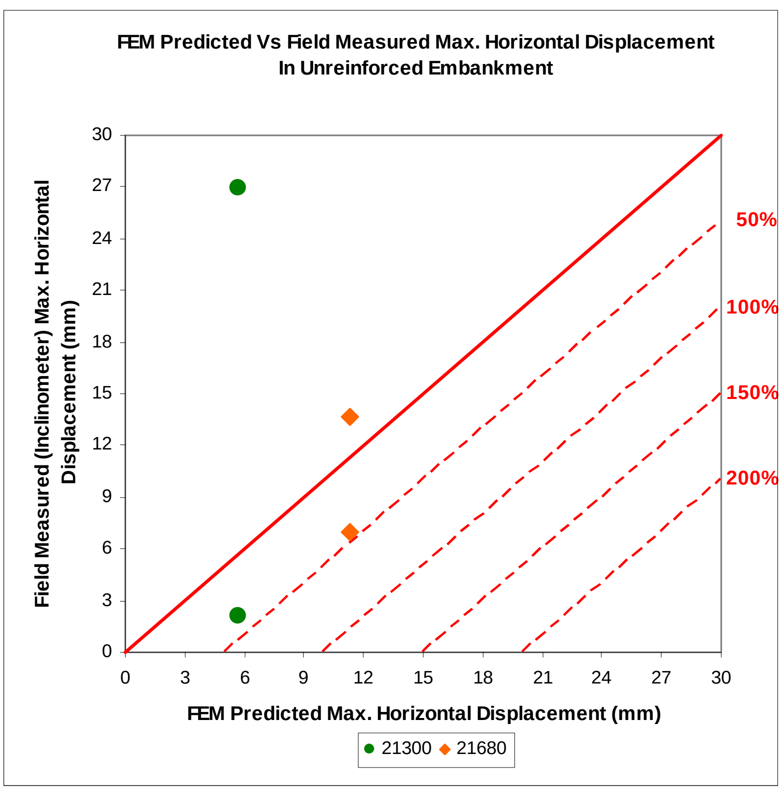

Figures 13: FEM vs Field measured horizontal displacements for unreinforced embankments

The figures above demonstrate that embankments BR19B and BR25A&B, which were reinforced with high strength woven geotextile, recorded smaller maximum lateral deflections measured by the field inclinometers compared to the lateral deflections computed by the finite element analysis. In the analysis, the models were built on the construction program in order to simulate the actual field conditions. The 2D Finite Element analysis over-estimated the maximum lateral deflection by 50% to 200%.

In the case of the embankments that were not reinforced with high strength woven geotextile (21+300 and 21+680), the results show that the maximum lateral deflections recorded in the field by inclinometers compares favorably to the values computed by the finite element analysis in the case of 21+680. However, there was a huge difference in the measurement by the inclinometer for section 21+300 with one of the measurement value (north bound) significantly higher than the predicted value.

It is noticeable from Table 4 that there is a significant difference in lateral deflections measured by the inclinometers at either end of the embankment toes. This can be explained in the case of embankments BR19B and 21+300. A detention basin was built along the north bound corridor to collect rainwater for construction use. The detention basin may well account for the difference in the north and south bound deflections with higher lateral displacement recorded at the north bound toes of the embankment. In addition, embankments BR25 A&B were constructed over an old channel which has been relocated. Again, this may account for the difference in north and south bound deflections. (It must be noted that the existence of detention basin and channel was not taken into account in the FE analysis).

It was also observed that the lateral displacements of the unreinforced embankments are significantly lower than those of the reinforced embankments. This difference in lateral displacements is the result of unreinforced embankments being founded on better foundation soil as illustrated in Figure 2.

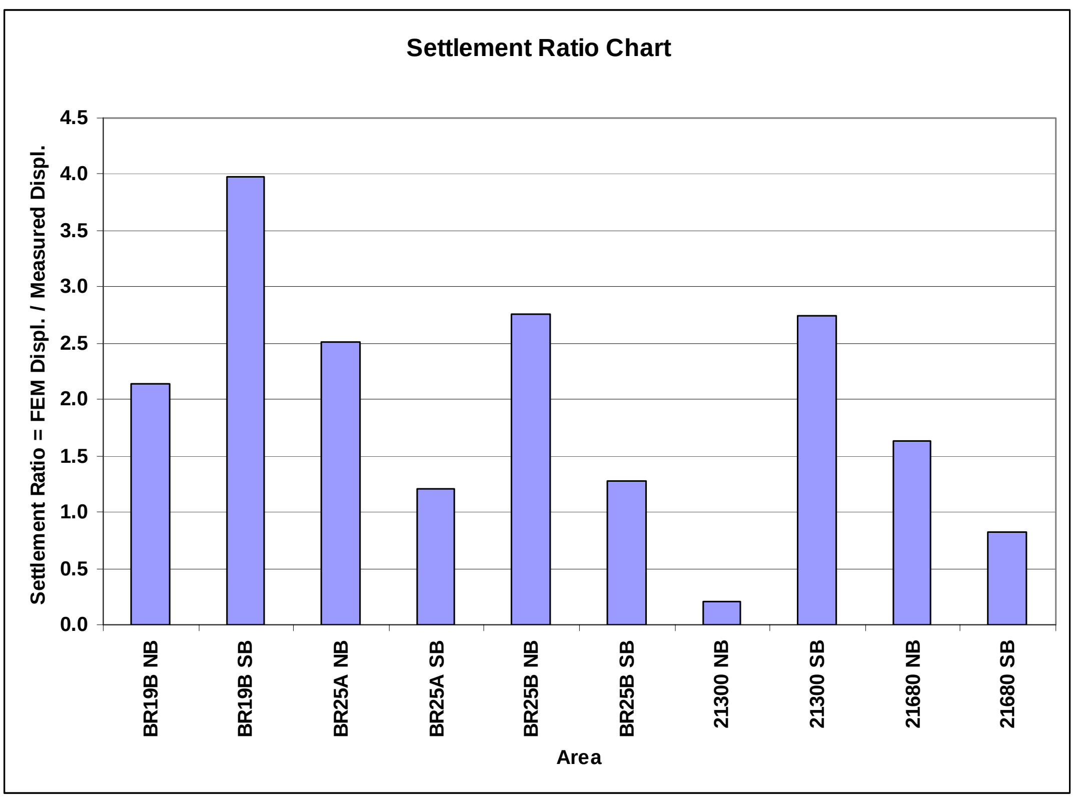

Figures 14: FEM Horizontal Displacements Vs Field Measured Horizontal Displacements
In order to examine the over-estimation of maximum lateral deflection recorded by the 2D finite element analysis compared to field recorded inclinometer readings, a settlement ratio is established and shown in Figure 14. Settlement ratio is quantified as 2D finite element predicted horizontal displacement divided by maximum lateral deflections measured by the field inclinometers.

From Figure 14, the settlement ratio ranging from 1.2 to 4.0 in reinforced embankments and 0.2 to 2.7 in unreinforced embankments.

## 7. CONCLUSIONS AND RECOMMENDATIONS

The reinforced embankments performed well with the assistance of additional tensile resistance provided by the high strength geotextile reinforcement with an evidence of substantial increased in settlement ratio ranging from 1.2 to 4.0. For the unreinforced embankments, a lower settlement ratio was recorded ranging from 0.2 to 2.7. The application of high strength geotextile enabled the embankment to be constructed at a higher construction rate and the lateral displacement to be controlled within the limits of the design.

2D finite element analysis generally produced conservative results for the high reinforced embankments overlying the soft soil which can be contributed by the conservative approach of BS 8006. A series of factors are applied to the short term tensile strength to produce the ultimate lateral strength required. As demonstrated on figures above, the over-estimation is generally ranging from 50% to 200%.

## ACKNOWLEDGEMENTS

The authors thank Maccaferri Australia, Polyfelt Asia and Coffey Geotechnics for providing all technical assistance in completing this paper. The work presented in this paper was carried out while the main author was supported by Leighton Abigroup Joint Venture. This support is greatly appreciated.

## REFERENCES

1. Wong, P.K, (2006), Preload Design, An Analytical Method Based On Bjerrum's Time Line Principle and comparison with other Design Methods, *Sydney Chapter 2006 Symposium*, Sydney AUSTRALIA.
2. Robertson, N, (1983), *Brisbane City: Gateway Bridge: Settlement Monitoring At Northern Approaches*, Reference MR625 140/8B/3, Brisbane, AUSTRALIA.
3. Department of Mines (1986), *Queensland Geology Map*, Sheet 9543, Brisbane, AUSTRALIA.
4. GHD (2002), *Gateway Motorway and Second River Crossing Planning Study – Volume 4 Appendix A to H*, Reference 140/U13/B, Brisbane, AUSTRALIA.
5. Queensland Department of Main Roads (2005), *Gateway Upgrade Project – Geotechnical Investigation – Northern Section Volume 1 to 4*, Reference R 3321, Brisbane, AUSTRALIA.
6. Connell Wagner (2006), *Gateway Upgrade Project, 110kV cable protection, Geotechnical Study,* Brisbane, AUSTRALIA.
7. Coffey Geotechnics, (2007), *Stage 2 Separable Portion B Construction Zone N4 Earthworks Embankment Design Report Ch 21200 – 22550*, Brisbane, AUSTRALIA.